Electronic Supplementary Material (ESI) for Journal of Materials Chemistry A.
This journal is © The Royal Society of Chemistry 2017

Bottom-up design of *de novo* thermoelectric hybrid materials using chalcogenide resurfacing

Ayaskanta Sahu,[a] Boris Russ,[a,b] Norman Su,[a,b] Jason D. Forster,[a] Preston Zhou,[a] Eun Seon Cho,[a] Peter Ercius,[c] Nelson E. Coates,[d] Rachel A. Segalman,[e] and Jeffrey J. Urban[a]*

[a]*The Molecular Foundry, Materials Sciences Division, Lawrence Berkeley National Lab, Berkeley, CA 94720, USA*

[b]*Department of Chemical and Biomolecular Engineering, University of California Berkeley, Berkeley, CA 94720, USA*

[c]*National Center for Electron Microscopy, Materials Sciences Division, Lawrence Berkeley National Lab, Berkeley, CA 94720, USA*

[d]*California Maritime Academy, Vallejo, CA 94720, USA*

[e]*Departments of Chemical Engineering and Materials, University of California Santa Barbara, Santa Barbara, CA 93106, USA*

[*]*email: jjurban@lbl.gov*

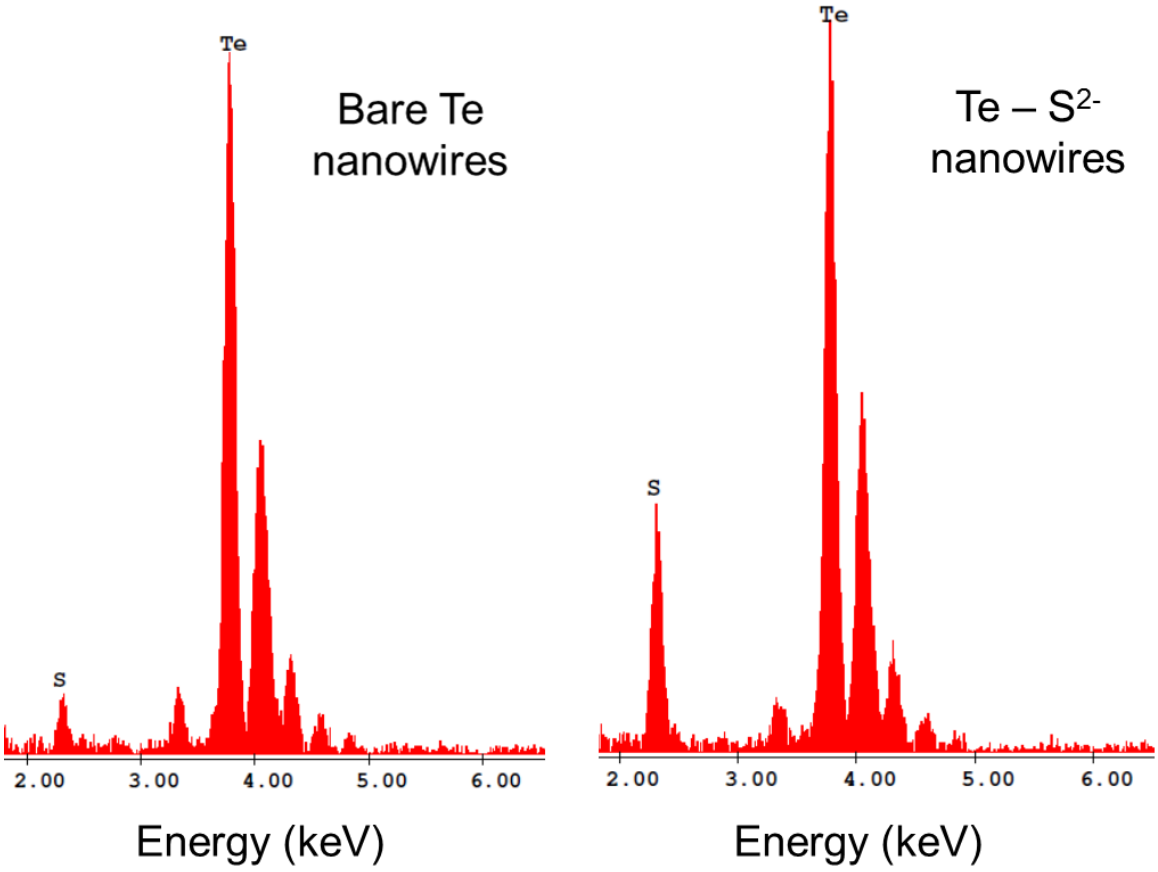

Figure S1. Energy Dispersive X-ray Analyses spectra acquired during SEM imaging, indicating presence of both tellurium from the nanowires and sulfur on the surface. A weak sulfur peak in the bare Te nanowires is due to sulfur impurities while a much stronger peak is observed in the doped nanowires (Te-S^{2-}). The spectra was obtained from a Te sample with average diameter of wires around 15 nm. Assuming 100% coverage of the surface Te atoms with S^{2-} atoms would give us only about 16% S-species in the samples. Quantifying by EDS gives us nearly 18% sulfur, which is pretty close to what one would expect with complete surface exchange.

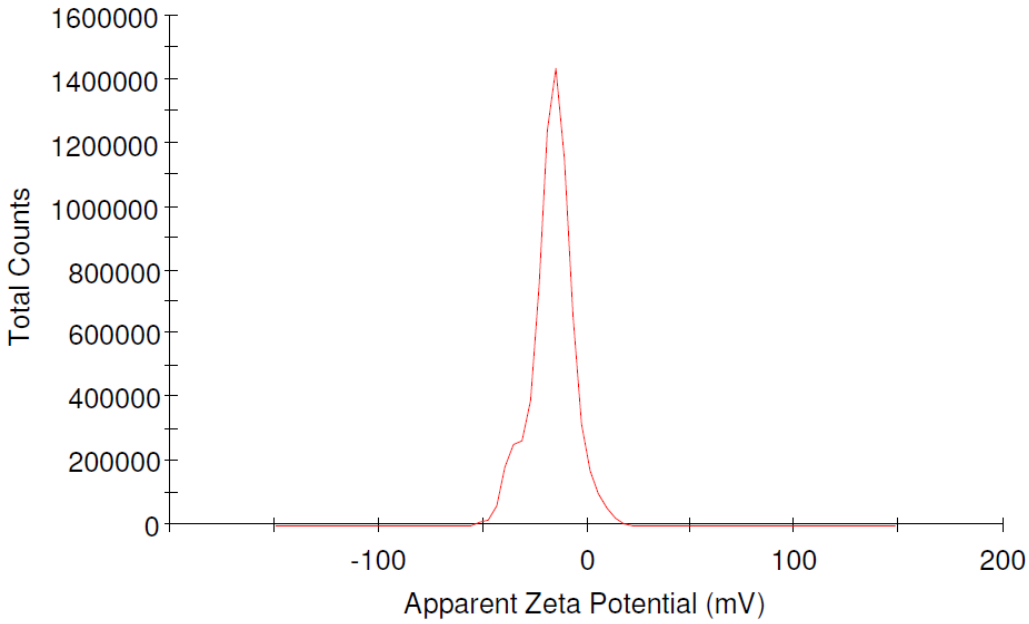

Figure S2. The averaged (n=72) Zeta Potential and phase distribution for sulfur capped tellurium nanowires dispersed in water. Sample concentration was ~10 microgram/mL. The sample was transferred to a zeta cell (Malvern Instruments) and measured at 25 °C. The zeta potential was -16.6 $\pm$ 10.2 mV (n=72). A viscosity of 0.8872 cP, a dielectric constant of 78.5 and Henry function of 1.5 were used for the calculations.

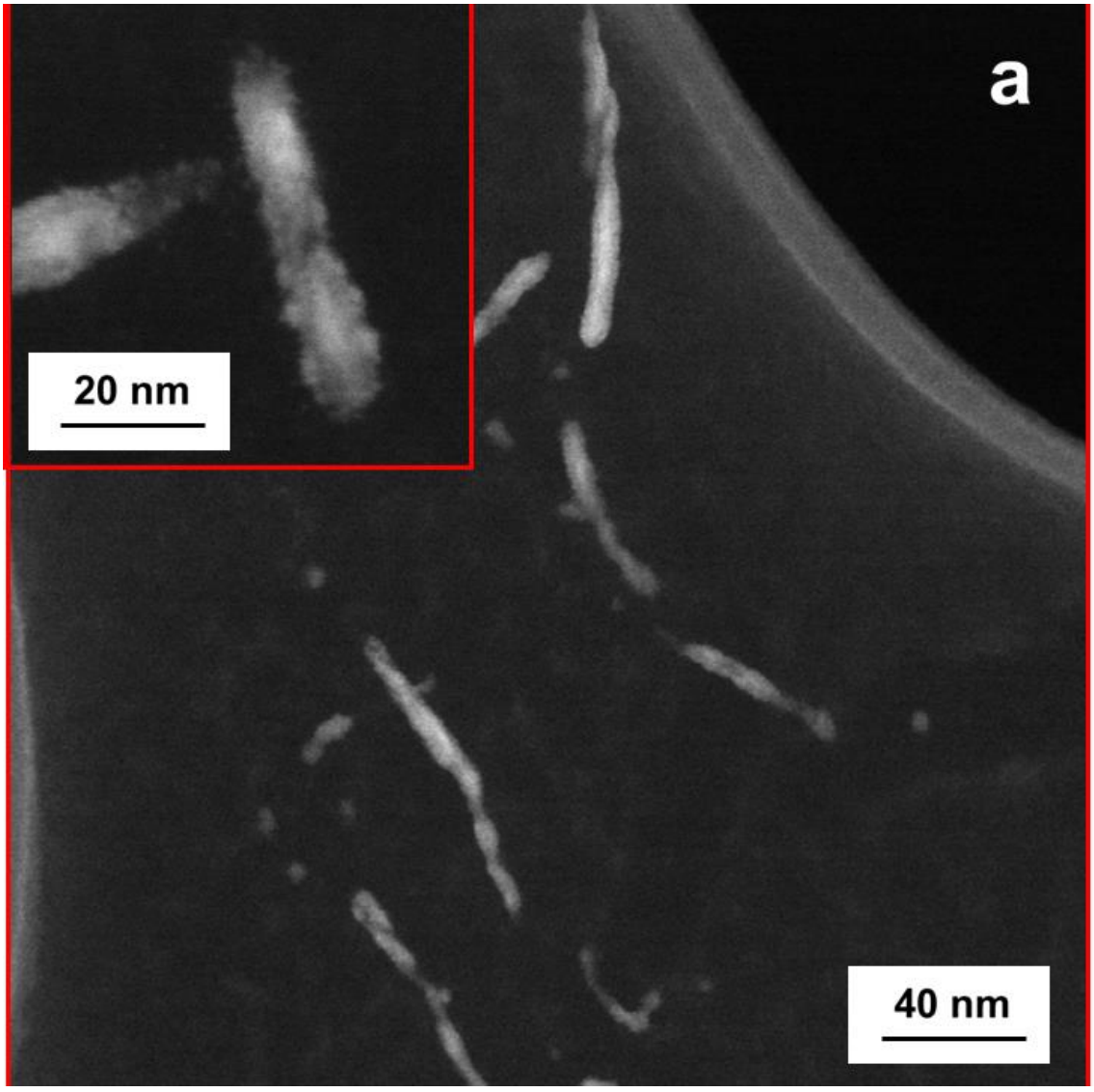
a
20 nm
40 nm

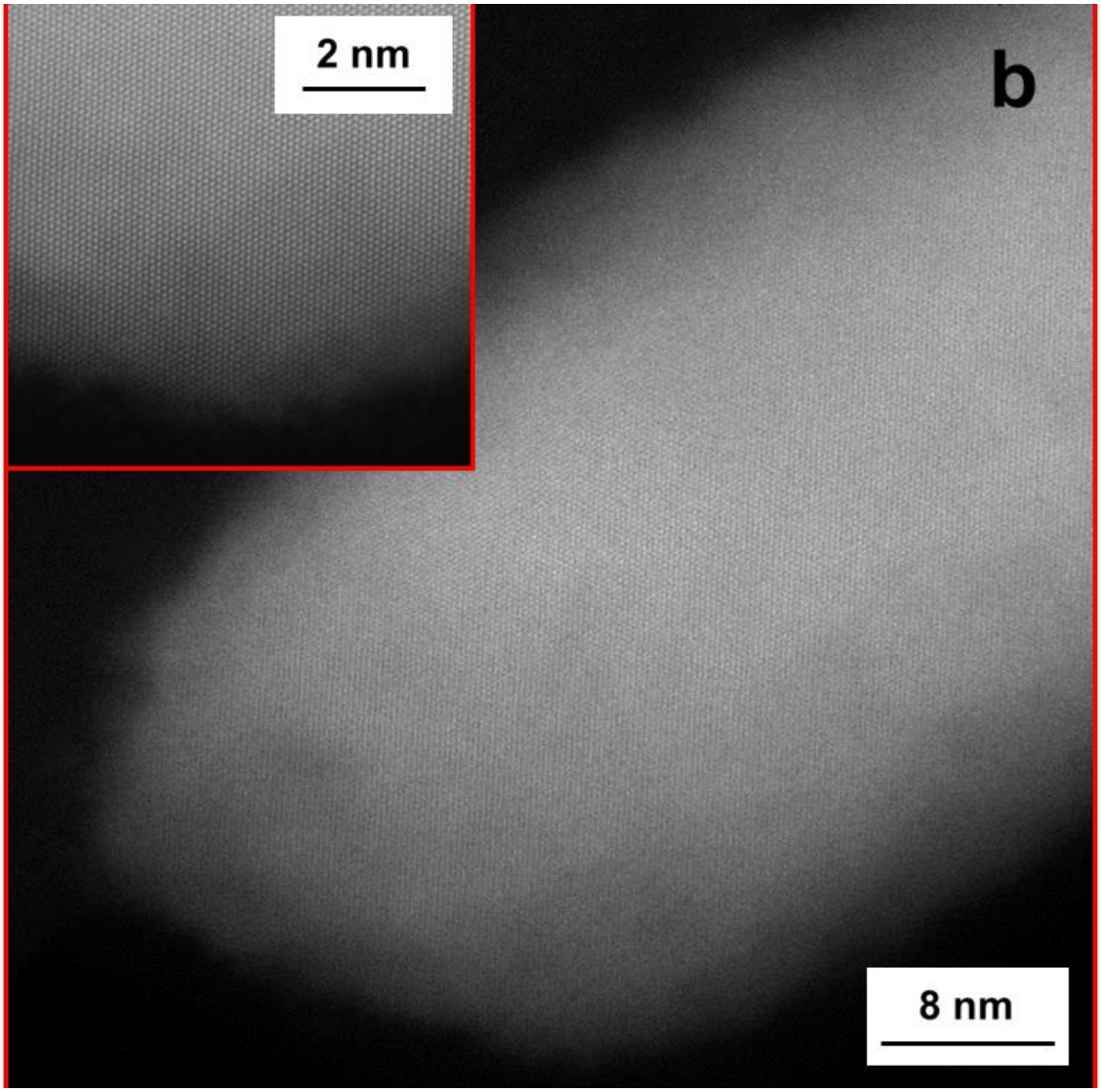

Figure S3. High resolution scanning transmission electron micrographs of (a) Te nanowires synthesized in-situ with PEDOT:PSS and (b) sulfur-capped Te nanowires synthesized without PEDOT:PSS. Insets show zoomed-in images of the respective nanostructures. While the nanowires that are synthesized ex-situ (without PEDOT:PSS during growth) are highly crystalline, the Te-PEDOT:PSS nanowires from an one-pot synthesis are polycrystalline.

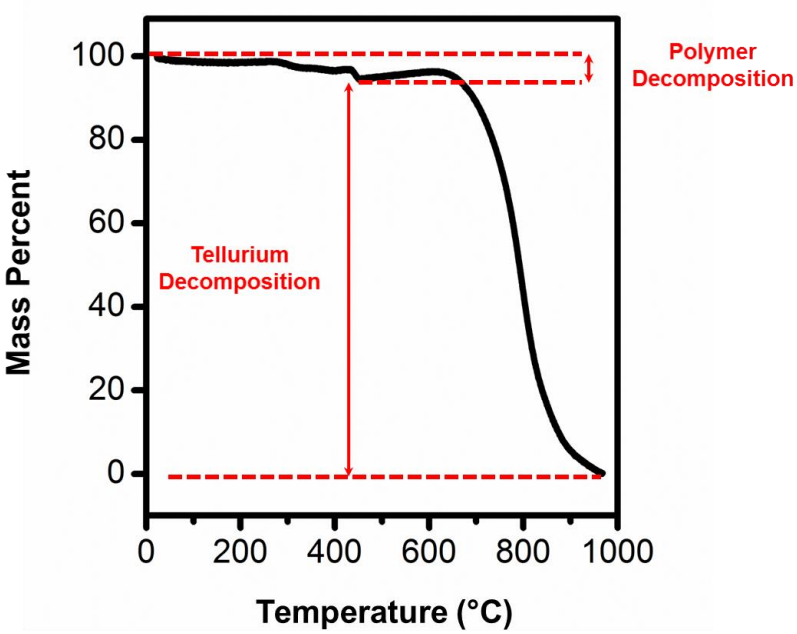

Figure S4. Thermogravimetric analyses (TGA) of the hybrid Te-PEDOT:PSS nanowires. The material was dried thoroughly before the TGA so there was no appreciable mass loss before 100 °C. There is a slight mass gain after the polymer has fully decomposed due to oxidation of the tellurium to tellurium dioxide.

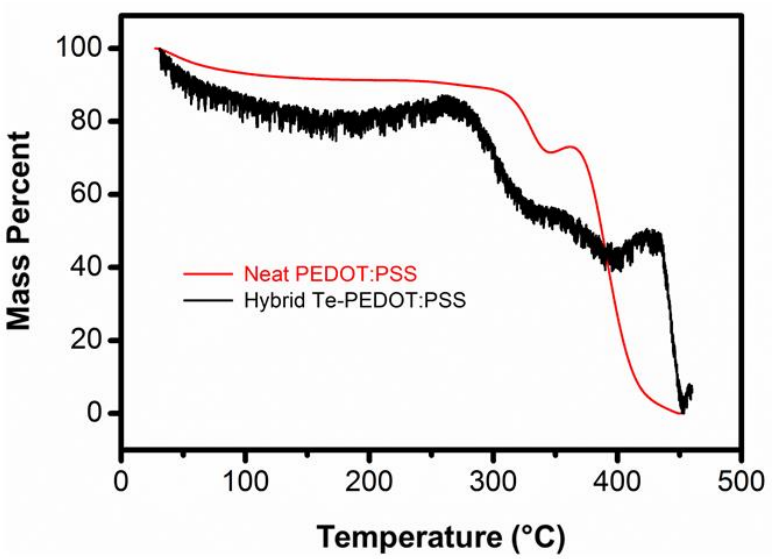

Figure S5: TGA of hybrid Te-PEDOT:PSS nanowires and neat PEDOT:PSS. Qualitatively both curves look similar. The data for the Te-PEDOT:PSS nanowires is noisier as compared to neat PEDOT:PSS since the absolute quantity of PEDOT:PSS in the hybrid sample is much smaller (~0.2-0.3 mg) as compared to neat PEDOT:PSS (~5 mg). The temperature at which PEDOT:PSS burns off the hybrid sample is a few degrees higher than neat PEDOT:PSS which might be due to the binding between the Te nanowire and the polymer.

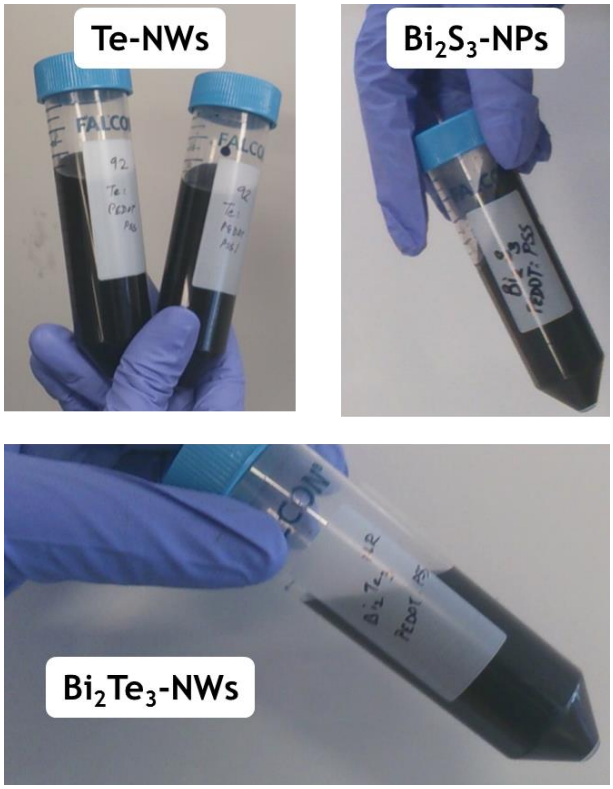

Figure S6. Stable dispersions of hybrid PEDOT:PSS-capped tellurium nanowires, bismuth sulfide nanoplatelets and bismuth telluride nanowires in water.

Figure S7. Smooth films cast from a series of dispersions of hybrid tellurium-PEDOT:PSS nanowires in water with varying amounts of PEDOT:PSS on 1cm X 1cm square glass substrates.

Discussion on Porosity in Films of Hybrid Nanowires:

Porosity is expected to play a big role when determining material and thermoelectric properties in these hybrid systems. For the as-synthesized nanowires with no PEDOT:PSS, we believe that porosity should exist when the wires are cast as thin films. As we coat these wires with PEDOT:PSS and add extra PEDOT:PSS for the hybrids, the excess PEDOT:PSS is expected to fill in the void space. However, quantifying the nanoporosity in these hybrid-systems is difficult and is the subject of ongoing work. When we report any thermoelectric property, **we report the values for the hybrid film which is going to be used as such in the thermoelectric device**. Thus, if we are underestimating the thermal conductivity due to film porosity, we are also underestimating the electrical conductivity.

Secondly, all the values are cited as weight percentages of tellurium. Converting it to volume percentages would result in the peak performance at nearly 50 volume % of polymer. At these high percentages, we believe that the film would be pretty dense with minimal void space. As reported by Coates et al., they expect porous films above 85% mass loading fraction of tellurium. Our maximum power factor is obtained at nearly 86% of tellurium. Thus we believe that we are almost close to fully dense films. We do not report any of our data as volume % since we do not actually measure the volume fraction during addition of the polymer or post deposition of the films; hence we stick to weight fractions which are measurable.

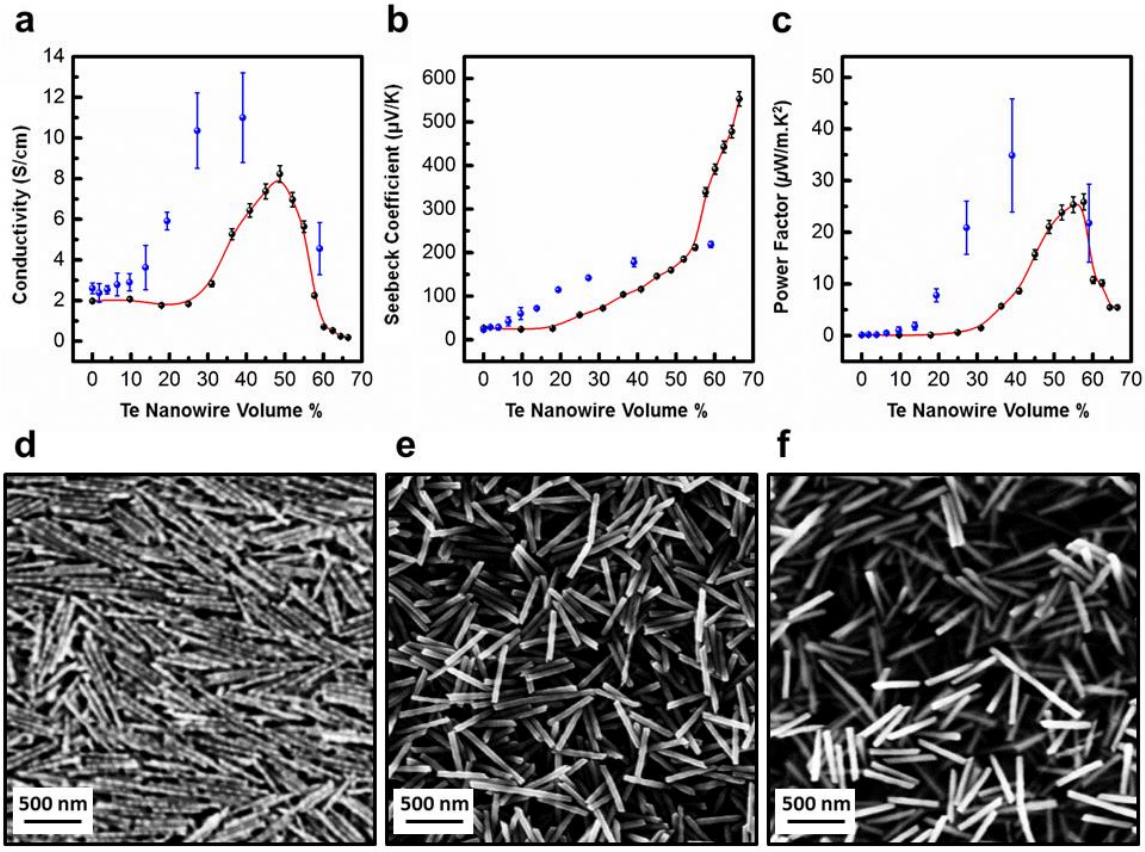

Figure S8. Dependence of (a) electrical conductivity, (b) Seebeck coefficient and (c) power factor on the volume percentage of tellurium (Te) nanowires in the hybrid film with PEDOT:PSS. The black markers represent the data from this report while the blue markers depict the data from Coates et al. (Ref. 35) for comparison. The red curve is a guide to the eye. Vertical error bars represent the variance of measurements over multiple samples. Horizontal error bars that represent the uncertainty in the volume percentage measurement are typically in the order of 5% and are not shown in the figure for clarity. Representative scanning electron microscopy images of hybrid Te nanowire-PEDOT:PSS films with Te nanowire volume percentages of (d) 65% (e) 43% and (f) 18%.

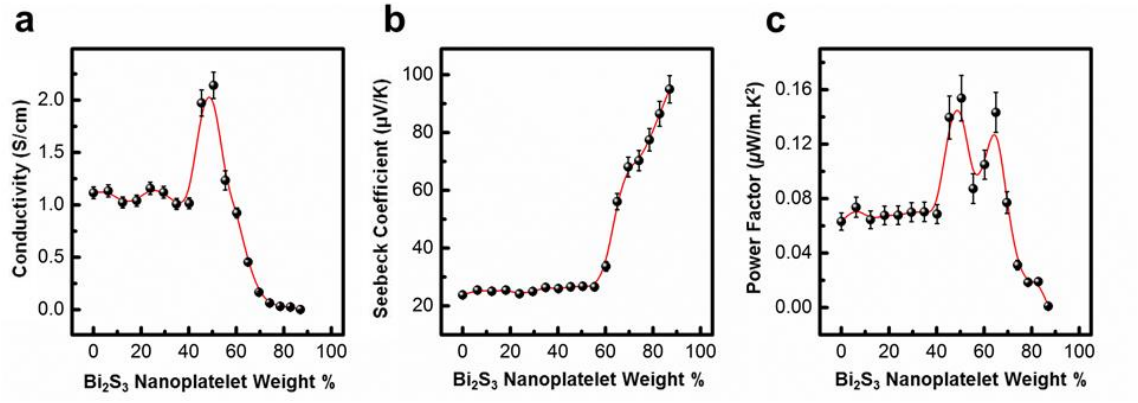

Figure S9. Dependence of (a) electrical conductivity, (b) Seebeck coefficient and (c) power factor on the weight percentage of bismuth sulfide nanoplatelets in the hybrid film with PEDOT:PSS. The red curve is a guide to the eye. Vertical error bars represent the variance of measurements over multiple samples. Horizontal error bars that represent the uncertainty in the weight percentage measurement are typically in the order of 5% and are not shown in the figure for clarity.

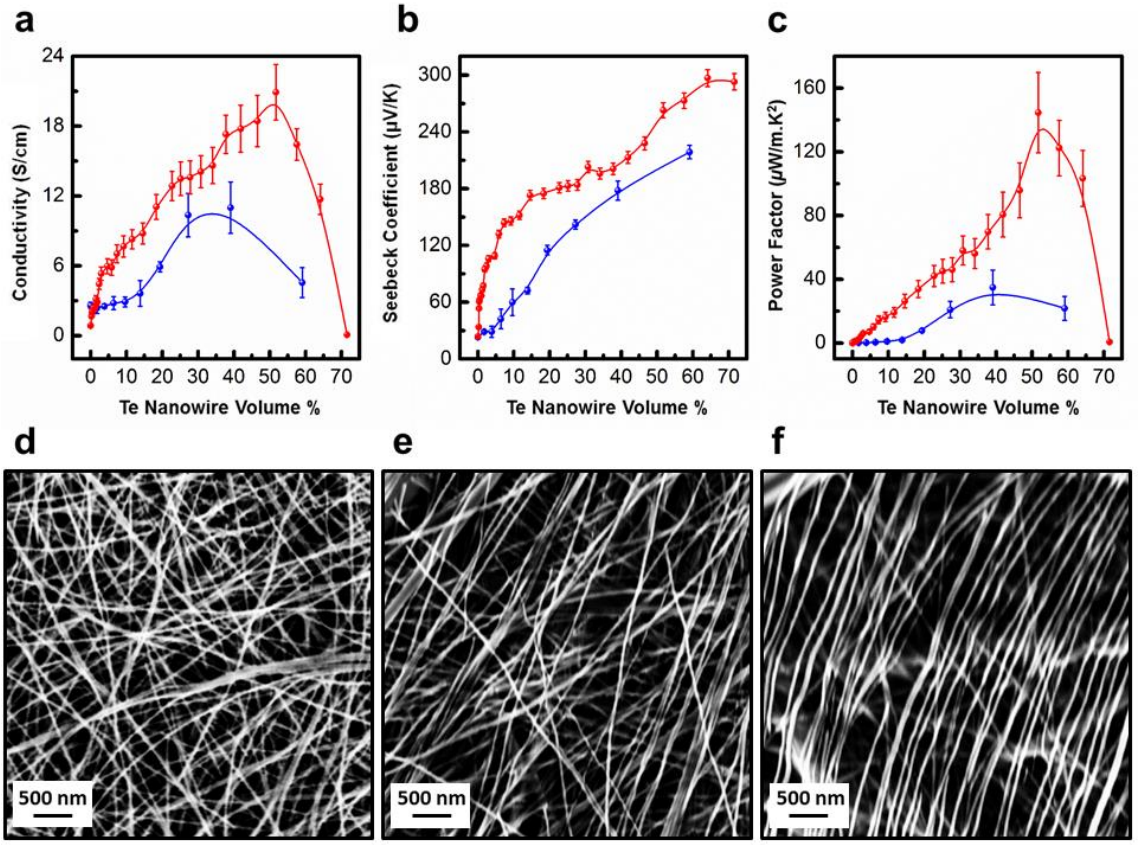

Figure S10. Dependence of (a) electrical conductivity, (b) Seebeck coefficient and (c) power factor on the volume percentage of tellurium (Te) nanowires in the hybrid film with PEDOT:PSS. The red markers represent the data from this report while the blue markers depict the data from the *in-situ* synthesis by Coates *et al.* (Ref. 35) for comparison. The red and blue curves are guides to the eye. Vertical error bars represent the variance of measurements over multiple samples. Horizontal error bars that represent the uncertainty in the volume percentage measurement are typically in the order of 5% and are not shown in the figure for clarity. Representative scanning electron microscopy images of hybrid Te nanowire-PEDOT:PSS films with Te nanowire volume percentages of (d) 70% (e) 45% and (f) 27%.

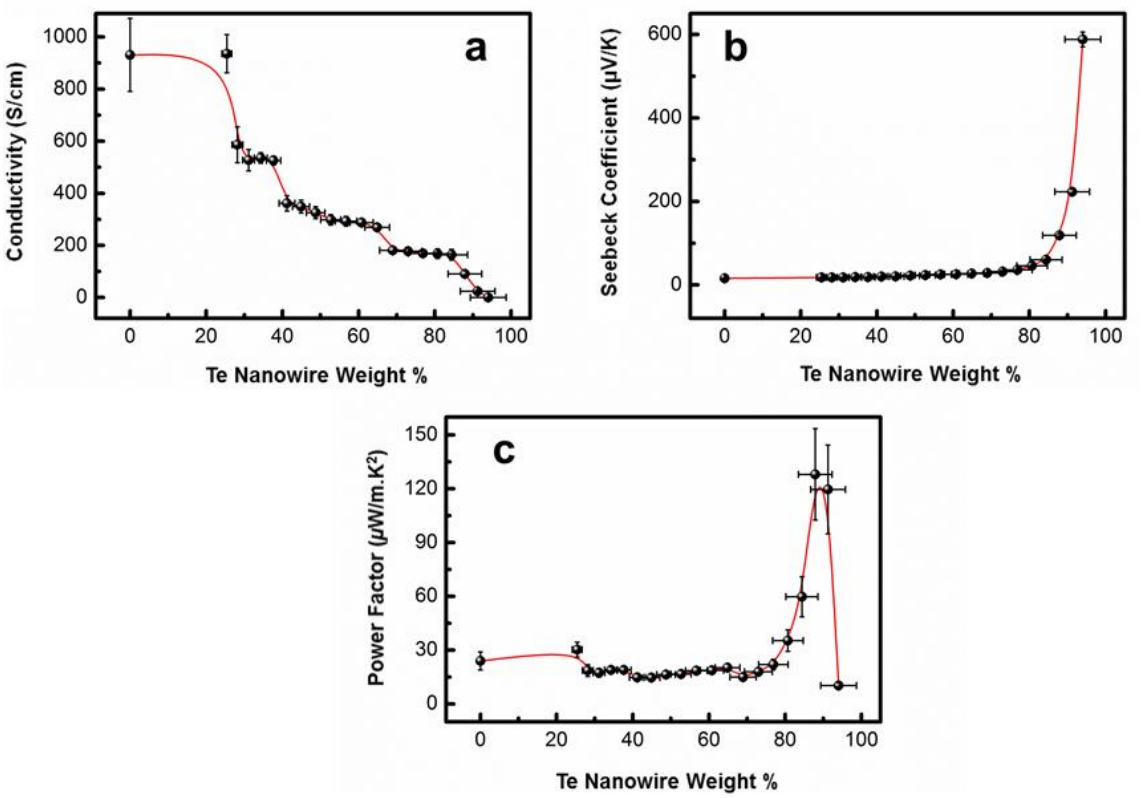

Figure S11. Dependence of (a) electrical conductivity, (b) Seebeck coefficient and (c) power factor on the weight percentage of tellurium nanowires in the hybrid film with PEDOT:PSS treated with formic acid. Vertical error bars represent the variance of measurements over multiple samples while horizontal error bars represent the uncertainty in the weight percentage measurement. The red curve is a guide to the eye.

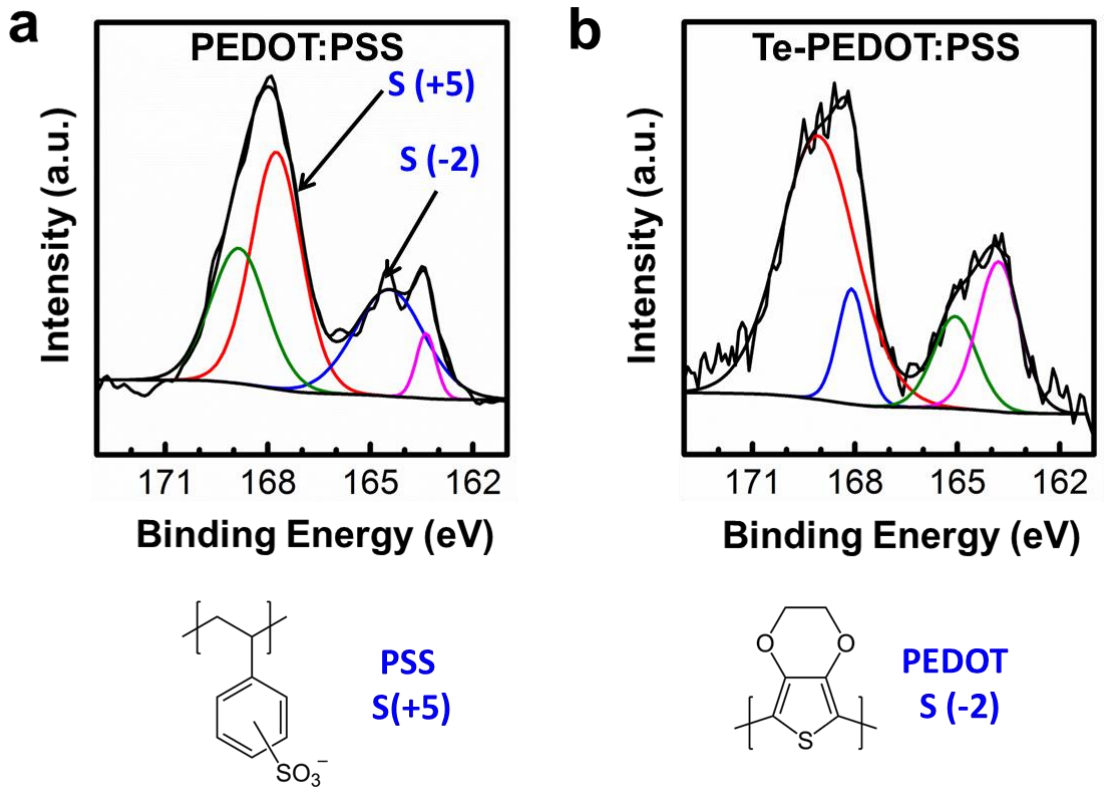

Figure S12. High-resolution XPS spectra of the S-2p peak of (a) PEDOT:PSS films, and (b) hybrid tellurium-PEDOT:PSS nanowire films in black. The green, red, blue and pink curves are the individual fits for different peaks with the smooth black curve representing the overall fit to the experimental obtained data. Curves were fit with quasi-Voigt lines following Shirley background subtraction. The two distinct peaks in (a) PEDOT:PSS centered around 164.5 eV and 169 eV can be attributed to signals obtained from PEDOT and PSS respectively. In contrast, the corresponding spectra for (b) Te-PEDOT:PSS hybrid nanowires shows a slightly higher fraction (~2%) of PEDOT peak as compared to the PSS peak.

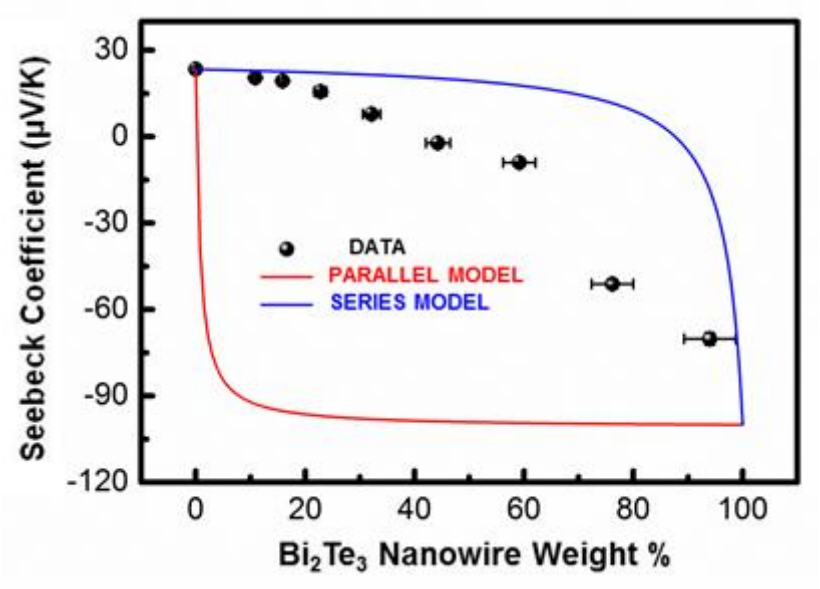

Figure S13. Dependence of Seebeck coefficient on the weight percentage of bismuth telluride (Bi_2Te_3) nanowires in the hybrid film with PEDOT:PSS. Horizontal error bars represent the uncertainty in the weight percentage measurement. Vertical error bars that represent the variance of measurements over multiple samples are captured within the data marker. The blue and red curves for the Seebeck coefficient data are from a series-connected and a parallel-connected two-component model.

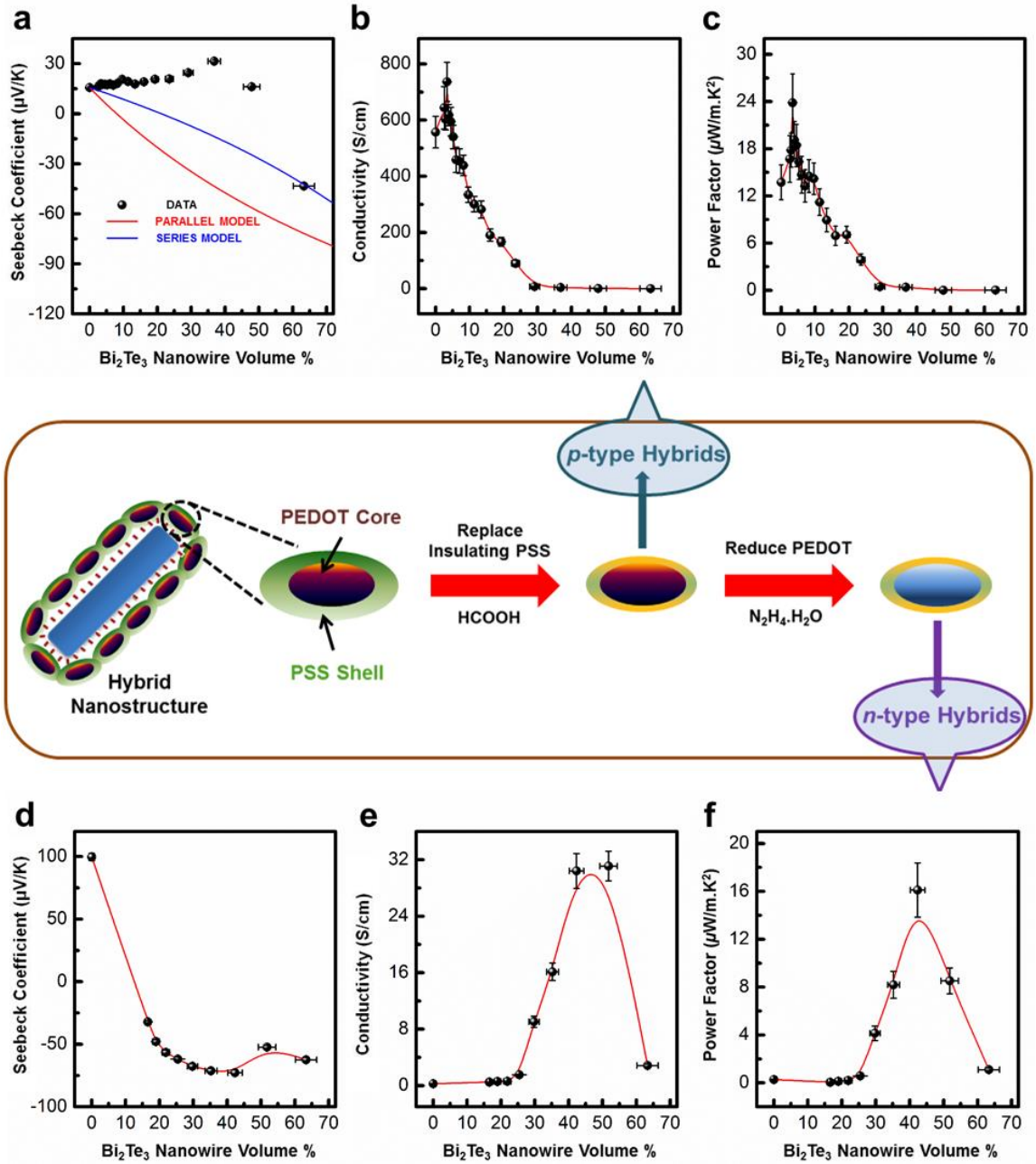

Figure S14. Scheme to obtain both *p*- and *n*-type Bi_2Te_3 hybrid nanostructures. Films of as-synthesized Bi_2Te_3-PEDOT:PSS nanowires are treated with formic acid to remove insulating PSS and generate high conductivity *p*-type hybrids (a-c) while those treated with formic acid followed by hydrazine hydrate result in *n*-type hybrids (d-f). Dependence of (a, d) Seebeck coefficient, (b, e) conductivity and (c, f) power factor on the volume percentage of bismuth telluride (Bi_2Te_3) nanowires in the *p*-type and *n*-type hybrid films respectively. Horizontal error bars represent the uncertainty in the volume percentage measurement. Vertical error bars represent the variance of measurements over multiple samples. For the Seebeck measurements, the vertical error bars are captured within the data marker. The blue and red curves for the Seebeck coefficient data in (a) are from a series-connected and a parallel-connected two-component model respectively. The red curves for the data in (b-f) serve as a guide to the eye.

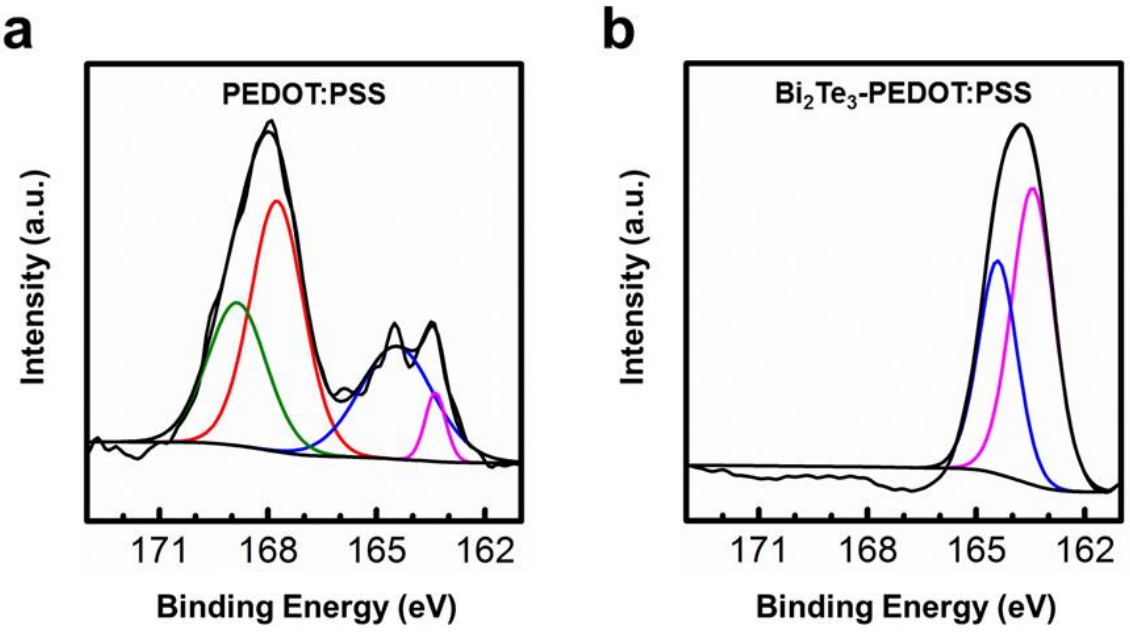

Figure S15. High-resolution XPS spectra of the S-2p peak of (a) PEDOT:PSS films, and (b) hybrid bismuth tellurium-PEDOT:PSS nanowire films treated with ethylene glycol followed by hydrazine hydrate in black. The green, red, blue and pink curves are the individual fits for different peaks with the smooth black curve representing the overall fit to the experimental obtained data. Curves were fit with quasi-Voigt lines following Shirley background subtraction. The two distinct peaks in PEDOT:PSS centered around 164.5 eV and 169 eV in (a) can be attributed to signals obtained from PEDOT and PSS respectively. In contrast, the corresponding spectra for bismuth telluride-PEDOT:PSS hybrid nanowires in (b) shows only one peak centered around 163.5 eV (PEDOT peak) ensuring complete removal of PSS from the as-cast films as well as *n*-type doping of PEDOT.